

# Feasibility of methylmethacrylate polymerization for bone cement by suspension polymerization in a gel phase

G. POLACCO, D. SEMINO, C. RIZZO

Department of Chemical Engineering, University of Pisa via Diotisalvi, 2-56126 Pisa, Italy

A thermo-kinetic model for a new suspension polymerization process to produce bone cement powder is developed. Polymerization is accomplished in a batch process in which the suspending phase is a gelled solution of water and agarose, which immobilizes the polymerizing particles all along the reaction. This "static" process is meant to produce polymethylmethacrylate particles of high purity, given that no suspending agent is needed, and of desired size. Owing to the absence of agitation, temperature profiles are of primary concern to ensure gel stability and desired molecular weight distributions. A reliable model is therefore required for the description of the basic thermal and kinetic phenomena and for reactor scale-up. The model predicts time and space profiles of temperature, conversion and polymer distributions. A good agreement with experimental data indicates that the model can be used with confidence in design and control studies.

## 1. Introduction

It is well known that the acrylic bone cement used in bone surgery is composed of very small spheres of polymethylmethacrylate (PMMA) and of a monomeric liquid phase (methylmethacrylate, MMA). The different commercial products are characterized by different qualities and quantities of initiators, accelerators and plastifiers and also by different comonomers which are added in order to improve the cement properties. The polymeric powder and the liquid are mixed by the surgeon in the surgery room and the polymerization takes place "in situ", i.e. between the bone and the metallic joint. The use of a prepolymerized phase is needed in order to minimize thermal effects and volume variations occurring during polymerization. It is therefore important to use a high polymer/monomer weight ratio, while making sure that the monomer is able to solve all the powder, so that the final product is highly uniform. The optimal in this respect is obtained when the average diameter of the spheres is around 60  $\mu\text{m}$ . That is why it is appropriate to perform a suspension polymerization in such a way that the polymer particles are produced directly with the appropriate size and shape. A common problem in this process is the tendency of the monomeric particles to coalesce and this takes place strongly particularly when the Trommsdorf effect is significant [1]. To ensure suspension stability, it is therefore necessary to use stabilizing agents, which need to be eliminated at the end of the process in order to guarantee the desired product purity.

In order to address this problem, a new polymerization technique has been accomplished. The interested reader can refer to the paper by Giusti *et al.* [2] for

a more detailed description of the process. A preliminary mixing is carried out to obtain a suspension of the monomer in a suspending phase composed of water and agarose. Then the suspending phase is transformed into a gel, so that the monomeric particles are kept at a fixed spatial position all along the polymerization process. In this way one avoids both coalescence and the presence of impurities in the product (agarose can be easily removed with hot water at the end of the process and it is, moreover, bio-compatible).

On the other hand, the thermal control of the process is worse than in the usual suspension polymerization and this constitutes a potential problem for the process. A study has therefore been undertaken in order to analyse the process feasibility. In particular, an appropriate thermo-kinetic model has been developed so that the influence of the system geometry and of the operating conditions on the temperature distribution can be evaluated.

## 2. Model development

From a macroscopic point of view, the system under analysis consists of a hemispheric reactor in which a huge number of monomer droplets are located at fixed spatial positions in the gel structure. After gelation is completed, the temperature is increased and polymerization starts in the imprisoned droplets.

Several models have been developed both for mass and for suspension polymerization [3, 4]. The peculiarity of this system is the fact that the individual droplets, in which a batch mass polymerization takes place, are embedded in a gel structure. This does not

allow any mixing and limits dissipation of the heat produced by the exothermic propagation step of the reaction. Consequently the reactor cannot have a uniform temperature.

Temperature profiles which are dependent on the heat flux through the reactor walls are of primary concern to determine local characteristics of the polymer produced. In order to obtain such profiles energy and material balances on a reacting droplet can be written, considering the droplet as a small batch reactor in which mass polymerization takes place. Following Chiu *et al.* [5], the balances on initiator  $I$ , monomer  $M$  (written in terms of conversion  $x$ ) and on the first three moments of the growing radicals ( $\lambda_0, \lambda_1, \lambda_2$ ) and of the dead polymer ( $\mu_0, \mu_1, \mu_2$ ) take the form:

$$\frac{dI}{dt} = -k_d I - \frac{\varepsilon I}{1 + \varepsilon x} \lambda_0 (1 - x) k_p \quad (1)$$

$$\frac{dx}{dt} = k_p (1 - x) \lambda_0 \quad (2)$$

$$\frac{d\lambda_0}{dt} = -\frac{\varepsilon \lambda_0^2}{1 + \varepsilon x} (1 - x) k_p + 2fk_d I - k_t \lambda_0^2 \quad (3)$$

$$\begin{aligned} \frac{d\lambda_1}{dt} = & -\frac{\varepsilon \lambda_1 \lambda_0}{1 + \varepsilon x} (1 - x) k_p + 2fk_d I - k_t \lambda_0 \lambda_1 \\ & + k_p \lambda_0 M_0 \frac{1 - x}{1 + \varepsilon x} \end{aligned} \quad (4)$$

$$\begin{aligned} \frac{d\lambda_2}{dt} = & -\frac{\varepsilon \lambda_2 \lambda_0}{1 + \varepsilon x} (1 - x) k_p + 2fk_d I - k_t \lambda_0 \lambda_2 \\ & + k_p M_0 \frac{1 - x}{1 + \varepsilon x} (2\lambda_1 + \lambda_0) \end{aligned} \quad (5)$$

$$\frac{d\mu_0}{dt} = -\frac{\varepsilon \mu_0 \lambda_0}{1 + \varepsilon x} (1 - x) k_p + k_{td} \lambda_0^2 + \frac{1}{2} k_{tc} \lambda_0^2 \quad (6)$$

$$\begin{aligned} \frac{d\mu_1}{dt} = & -\frac{\varepsilon \mu_1 \lambda_0}{1 + \varepsilon x} (1 - x) k_p + k_{td} \lambda_0 \lambda_1 \\ & + k_{tc} \lambda_0 \lambda_1 \end{aligned} \quad (7)$$

$$\begin{aligned} \frac{d\mu_2}{dt} = & -\frac{\varepsilon \mu_2 \lambda_0}{1 + \varepsilon x} (1 - x) k_p + k_{td} \lambda_0 \lambda_2 \\ & + k_{tc} (\lambda_0 \lambda_2 + \lambda_1^2) \end{aligned} \quad (8)$$

where  $k_d, k_p, k_t, k_{tc}, k_{td}$  are the kinetic constants for initiator decomposition, propagation, termination, termination by combination and termination by disproportionation ( $k_t = k_{tc} + k_{td}$ ) and  $M_0$  is the initial monomer concentration in the droplets.

Here  $\varepsilon = (\rho_m - \rho_p)/\rho_p$  is the volume expansion factor;  $\rho_m$  and  $\rho_p$  are the monomer and polymer densities, respectively. An energy balance could be written as well, but has been neglected as the droplet thermal behaviour will be considered in a global energy balance.

The number average molecular weight  $M_n$  and weight average molecular weight  $M_w$  can be computed from the moments of the distributions as

$$M_n = \frac{\lambda_1 + \mu_1}{\lambda_0 + \mu_0} \quad M_w = \frac{\lambda_2 + \mu_2}{\lambda_1 + \mu_1} \quad (9)$$

As conversion in the reacting mixture reaches high values, gel and glass effect are included in the kinetic constants through appropriate parameters. The correlations developed for MMA polymerization by Chiu *et al.* [4] have been chosen. The propagation and termination kinetic constant are therefore computed as follows:

$$\frac{1}{k_t} = \frac{1}{k_{t0}} + \vartheta_t(T) \frac{\lambda_0}{\exp \left[ \frac{2.303 \phi_m}{A(T) + B\phi_m} \right]} \quad (10)$$

$$\frac{1}{k_p} = \frac{1}{k_{p0}} + \vartheta_p(T, I_0) \frac{\lambda_0}{\exp \left[ \frac{2.303 \phi_m}{A(T) + B\phi_m} \right]} \quad (11)$$

$$\phi_m = \frac{1 - x}{1 + \varepsilon x} \quad (12)$$

$$\vartheta_p = \frac{\vartheta_p^0}{I_0} \exp \left( \frac{E_{\vartheta p}}{RT} \right) \quad \vartheta_t = \vartheta_t^0 \exp \left( \frac{E_{\vartheta t}}{RT} \right) \quad (13)$$

$$A(T) = C_1 - C_2(T - T_{gp})^2 \quad (14)$$

where  $\vartheta_p, \vartheta_t, A$  and  $B$  are the gel and glass effect parameters.

Looking at the global system, one can write the energy balance in spherical coordinates as follows:

$$\frac{\partial T}{\partial t} = \frac{1}{\rho c_p} \frac{1}{r^2} \frac{d}{dr} \left( r^2 k \frac{\partial T}{\partial r} \right) + \frac{Se}{\rho c_p} \quad (15)$$

where  $Se$  represents the heat generation term per unit volume.  $K$  and  $c_p$  in Equation 15 are averages values of thermal conductivity and thermal capacity, respectively, and are computed as follows:

$$K = (1 - \gamma)K_{H_2O} + \gamma x K_{PMMA} + \gamma(1 - x)K_{MMA} \quad (16)$$

where

$$\gamma = \varepsilon_\sigma(1 + \varepsilon x) \quad (17)$$

and  $\varepsilon_\sigma$  is the volumetric fraction of the reacting droplets, defined as:

$$\varepsilon_\sigma = \left( \frac{V_{MMA}}{V_{MMA} + V_{water}} \right)_{t=0} \quad (18)$$

$$\rho c_p = \left( \frac{(\rho c_p)_{H_2O} W_{H_2O} + (\rho c_p)_{MMA} W_{MMA}}{W_{H_2O} + W_{MMA}} \right)_{t=0} \quad (19)$$

and  $W_{H_2O}, W_{MMA}$  are the weight fractions of water and MMA.

It has been assumed here that a single variable  $T(r, t)$  describes both the temperature in the gel phase and in the reacting particles: this means that a quasi-steady-state assumption has been made by which the reacting droplets are constantly considered at thermal equilibrium with the surrounding gel. This is justified by the high surface to volume ratio in particles, which makes the local heat transfer very fast as compared to the process time scale. Spheric symmetry is maintained by considering the heat flux on the top of the hemisphere negligible.

In order to write the dependence of the generation term from the droplet composition, one has to consider moreover that the particle states are function not

only of the time  $t$  but also of the radius  $r$  at which the droplet is located. The balances (Equations 1–8) have to be formally rewritten by substituting the total derivatives with respect to time with partial derivatives. The heat generation term takes therefore the form:

$$Se(r, t) = \Delta H_r \varepsilon_\sigma M_0 k_p (1 - x(r, t)) \lambda_0(r, t) \quad (20)$$

where  $\Delta H_r$  is the heat of reaction.

The system to be solved turns out to be composed of nine coupled partial differential equations, which describe the time and space profiles of temperature, initiator concentration, conversion and of the leading moments of the growing radicals and of the dead polymers.

The main interest lies in analysing how the main design parameters (reactor surface to volume ratio, volumetric fraction of the reacting phase, jacket temperature) affect the radial temperature profile during reaction and the molecular weight distribution of the polymer produced in the different particles.

### 3. Results and discussion

The temperature profiles, which are obtained with the model developed here, are compared with experimental temperature data relative to MMA polymerization in a glass hemispheric reactor with a refrigerating jacket. Benzoyl peroxide has been chosen as the initiator and a weight ratio of 4/1 between the suspending phase and the monomeric one has been used; the reactor volume is  $V = 0.5$  l. After the suspending phase has become a gel ( $T = 40^\circ\text{C}$ ), water has been fed to the jacket at a constant temperature  $T_c = 70^\circ\text{C}$  and has no longer been changed during reaction. Four thermocouples have been used to measure the temperature profiles at different radial positions; the measurements are shown in Fig. 1 (note that the thermocouple reference number increases as the radius decreases, as schematically shown on the lower right side, and that the same reference numbers/symbols are used for Figs 1–6). There is clearly a gradual increase of the temperature starting from the

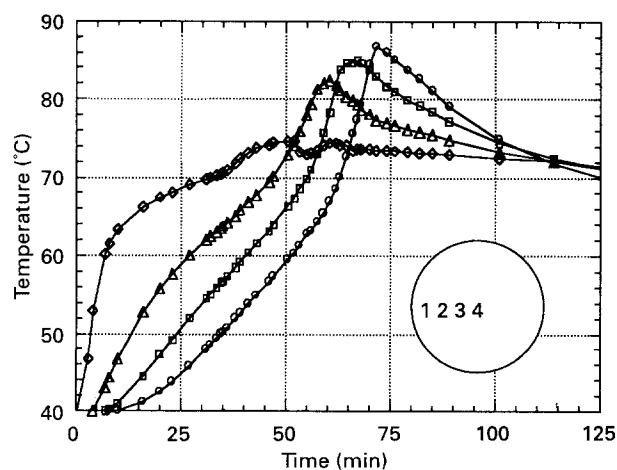


Figure 1 Experimental temperature data for the hemispheric reactor.  $\diamond$  Thermocouple (TC) 1;  $\triangle$  TC 2;  $\square$  TC 3;  $\circ$  TC 4.

outside and then propagating to the inside of the reactor, which causes reaction to start and develop. Temperature peaks are higher in the inner part of the reactor where the heat transmission is more difficult; the temperature values are anyway reasonable everywhere: no run-away occurs and the temperature limit for the stability of the gel ( $T = 90^\circ\text{C}$ ) is not reached.

The same experiment has been simulated using the model. The inherent physical and kinetic parameters, which have been taken from the literature, are reported in Table I (temperatures are in degrees Kelvin). The model has been therefore integrated assuming, as initial conditions, uniform temperature and concentrations ( $T_0 = 40^\circ\text{C}$ ,  $I_0 = 0.2$  mol/l,  $M_0 = 9.26$  mol/l) and setting conversion and all the polymer moments to zero.

The parameter on which the largest uncertainty is expected is the average thermal conductivity, for two main reasons. The first is that the system is surely not homogeneous, so that heat conduction proceeds quite differently in the reacting droplets and in the suspending phase. The second is that, even if the gel is static from a macroscopic point of view, this is not true at a microscopic scale, particularly when operating close to the limits of the gel stability region. Qualitative agreement with the experimental results is obtained using conductivity data from the literature and Equation 16, but to achieve a good quantitative agreement (Fig. 2) a multiplicative coefficient for conductivity ( $\alpha = 1.65$ ) has been included, in order to take into account microscopic mobility of the water molecules in the gel phase.

Even closer agreement with experimental data is obtained when a dependence of average conductivity on temperature is considered, to account for an increase of mobility with temperature. The results in Fig. 3 correspond to a quadratic dependence:  $K = K(T_0) \times (1 + \alpha(T - T_0)^2)$  where  $\alpha = 6 \times 10^{-4}$ .

Figs 4 and 5 show, for this latter case, conversion and molecular weight profiles at the same four radial positions. As expected from the physical understanding of the process, conversion proceeds from the outside to the inside, where the profiles are steeper in the Trommsdorf effect region due to the temperature peaks.

As far as molecular weights are concerned, in the outer part of the reactor, where the temperature profile is almost flat, so are the molecular weight profiles before the above mentioned effect takes place. When it is relevant, an increase in molecular weight is caused by the decrease of the termination kinetic constant. In the inner parts of the reactor a second counteracting effect is present as well. When the Trommsdorf effect takes place, the temperature increase causes molecular weight to fall. The increase in molecular weights therefore becomes smaller going from the outside to the inside, where it is almost absent. From an overall point of view, the system heterogeneity causes the breadth of the molecular weight distribution to increase as compared to the usual suspension process. This is in agreement with the experimental data [2]. Such good results make it possible to use the model with confidence to predict the behaviour of a reactor

TABLE I Physical and kinetic parameters

$K_d$ ( $\text{min}^{-1}$ )	$6.32 \times 10^{16} \exp[-1.543 \times 10^4/T]$
$K_{p,0}$ ( $\text{l min}^{-1} \text{mol}^{-1}$ )	$2.95 \times 10^7 \exp[-4.353 \times 10^3/(1.987T)]$
$K_{t,0}$ ( $\text{l min}^{-1} \text{mol}^{-1}$ )	$5.88 \times 10^9 \exp[-7.01 \times 10^2/(1.987T)]$
$K_{tc,0}$ ( $\text{l min}^{-1} \text{mol}^{-1}$ )	0.0
$g_p^0$ (min)	$5.54 \times 10^{-16}$
$g_t^0$ ( $\text{min mol l}^{-1}$ )	$1.15 \times 10^{-22}$
$E_{a,p}$ ( $\text{cal mol}^{-1}$ )	$2.7813 \times 10^4$
$E_{a,t}$ ( $\text{cal mol}^{-1}$ )	$3.4765 \times 10^4$
$B$	$3 \times 10^{-2}$
$C_1$	$1.68 \times 10^{-1}$
$C_2$ ( $\text{K}^{-2}$ )	$8.21 \times 10^{-6}$
$T_{sp}$ (K)	387
$f$	0.6
$\rho_{\text{H}_2\text{O}}$ ( $\text{g cm}^{-3}$ )	1.0
$\rho_{\text{MMA}}$ ( $\text{g cm}^{-3}$ )	$0.973 - 1.164 \times 10^{-3} [T - 273]$
$\rho_{\text{PMMA}}$ ( $\text{g cm}^{-3}$ )	1.2
$c_{p,\text{H}_2\text{O}}$ ( $\text{cal mol}^{-1} \text{K}^{-1}$ )	18
$c_{p,\text{MMA}}$ ( $\text{cal mol}^{-1} \text{K}^{-1}$ )	40
$K_{\text{H}_2\text{O}}$ ( $\text{cal mol}^{-1} \text{K}^{-1} \text{min}^{-1}$ )	$8.33 \times 10^{-2} + 1.67 \times 10^{-4} (T - 273)$
$K_{\text{MMA}}$ ( $\text{cal mol}^{-1} \text{K}^{-1} \text{min}^{-1}$ )	$(2.856 \times 10^3/T)[9.665 \times 10^{-3} - 1.1 \times 10^{-5}(T - 273)]^{4/3}$
$K_{\text{PMMA}}$ ( $\text{cal mol}^{-1} \text{K}^{-1} \text{min}^{-1}$ )	$2.23 \times 10^{-2}$
$\Delta H_r$ ( $\text{cal mol}^{-1}$ )	$1.3 \times 10^4$

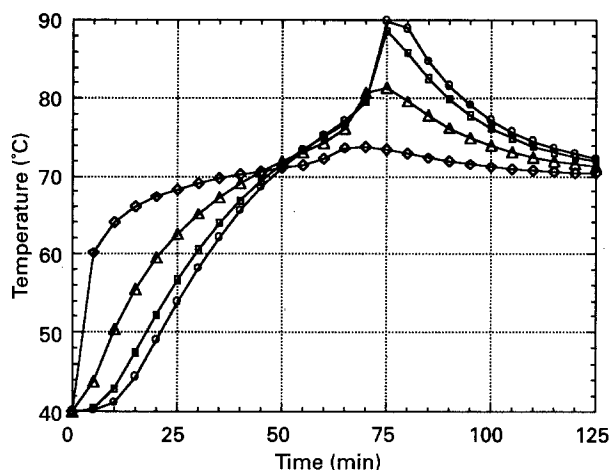


Figure 2 Computed temperature profiles (including a multiplicative coefficient for conductivity).  $\diamond$  Thermocouple (TC) 1;  $\triangle$  TC 2;  $\square$  TC 3;  $\circ$  TC 4.

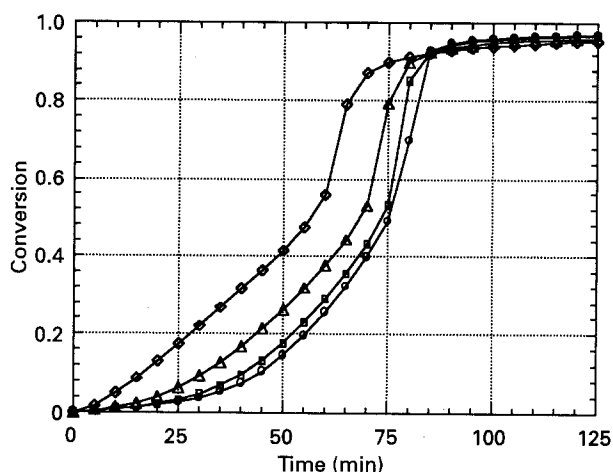


Figure 4 Computed conversion profiles.  $\diamond$  Thermocouple (TC) 1;  $\triangle$  TC 2;  $\square$  TC 3;  $\circ$  TC 4.

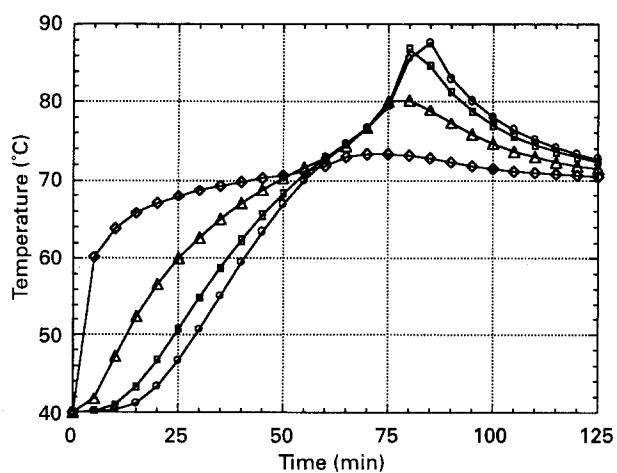


Figure 3 Computed temperature profiles (including quadratic dependence of average conductivity on temperature).  $\diamond$  Thermocouple (TC) 1;  $\triangle$  TC 2;  $\square$  TC 3;  $\circ$  TC 4.

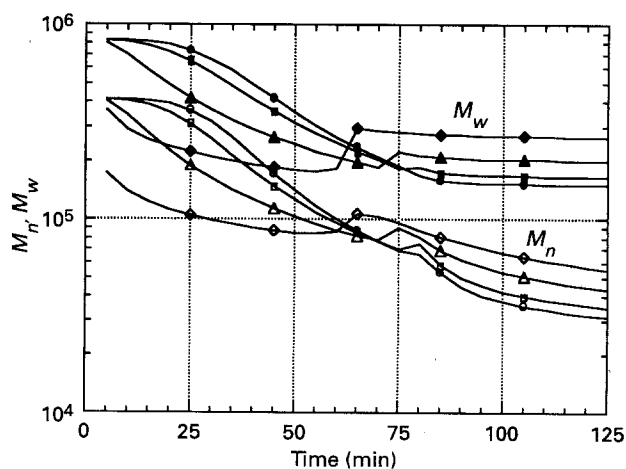


Figure 5 Computed number and weight average molecular weights.  $\diamond$  Thermocouple (TC) 1;  $\triangle$  TC 2;  $\square$  TC 3;  $\circ$  TC 4.

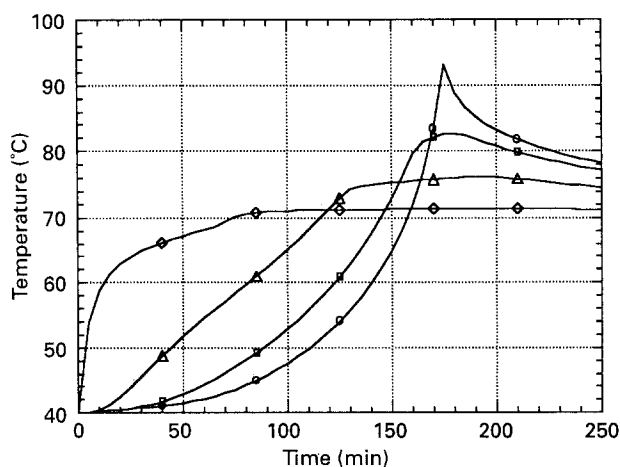


Figure 6 Computed temperature profiles for the cylindrical reactor.  $\diamond$  Thermocouple (TC) 1;  $\triangle$  TC 2;  $\square$  TC 3;  $\circ$  TC 4.

with different size and shape, where the same reactions take place.

A cylindrical reactor with a radius  $r = 10$  cm and a length such that cylindrical symmetry is maintained has been tested. With the same parameters of the previous case, the results shown in Fig. 6 have been obtained. It is important to point out that in this case the reaction is slower and the temperatures peaks are higher. In particular, in the inner part of the reactor temperature goes beyond the values for which gel stability is guaranteed. If this is the case, one has to design a control system, which operates on the jacket temperature, that is able to make reaction start at the beginning and then maintains the peaks under the permitted limits during operation.

Such results are promising if one considers that on the one hand the production of PMMA for bone cements is quite limited in quantity (so that big reactors are not required) and on the other hand that a number of design solutions can be implemented in order to keep the maximum temperature low. Higher heat fluxes can be obtained by using metallic reactors or adding inner exchange surfaces. Moreover, a lower heat generation per unit volume can be obtained if the water/monomer weight ratio is increased.

An industrial production would need an effective temperature control system that manages to keep temperature profiles as smooth as possible in order to avoid run-away and to guarantee a product with uniform properties. Such control system is the subject of further research.

#### 4. Conclusions

A detailed model that describes suspension polymerization of MMA in a gel phase to produce bone cement powder has been validated by comparison with experimental results. Time and space profiles of temperature, conversion and polymer distributions have been obtained by solving a system of partial differential equations in which Trommsdorf and glass effects have been considered and heat dispersion by conduction in the gel phase has been carefully described. The problems caused by the temperature peaks in the reactor have been highlighted and possible design and control solutions investigated.

The good agreement with experimental results suggest the use of the model both in design and in control studies.

#### Acknowledgments

The authors gratefully thank Mr M. Palla for his helpful suggestions in the preparation of the manuscript.

#### References

1. E. H. TROMMSDORF, H. KOLHE and P. LAGANG, *Macromol. Chem.* **1** (1948) 169.
2. P. GIUSTI, M. PALLA, G. PIZZIRANI, G. POLACCO and C. RIZZO, in Proceedings of the 11th European Society for Biomaterials Congress, Pisa, Italy, September 1994.
3. H. G. YUAN, G. KALFAS and W. H. RAY, *J. Macromol. Sci C31* (1991) 215.
4. G. KALFAS, H. G. YUAN and W. H. RAY, Preprint of paper presented at 1991 Annual AIChE Meeting, Los Angeles, November 1991.
5. W. Y. CHIU, G. M. CARRAT and D. S. SOONG, *Macromolecules* **16** (1983) 348.